Comparison of various cusp models with high- and low-resolution observations

M. Yamauchi (yama@irf.se) and R. Lundin
Swedish Institute of Space Physics, Kiruna, Sweden

Abstract. Three major cusp models are systematically compared with low-resolution (large-scale) and high-resolution (fine-scale) low-altitude observations. Those models are (a) global magnetohydrodynamics (MHD) models (including MHD+drift models), (b) turbulent/diffusive entry models, and (c) direct flowing entry models. Although low resolution data are mostly consistent with MHD models, high-resolution data mostly contradicts them. The data instead supports the other models in which the cusp is considered as a local "extra" open region. This is a good lesson to us: past supportive "tests" of MHD cusp models might have essential flaws in the methodology, and high-resolution data is necessary even for large-scale modelings.

Keywords: test of models, cusp, direct entry, MHD, drift, local, high-resolution data

Accepted version, Space Science Reviews (2001)
Yamauchi, M., and Lundin, R. (2001): Comparison of various cusp models with high- and low-resolution observations, Space Sci., Rev., 95, 457-468, doi: 10.1023/A:1005237630306.

1. Introduction

Since its finding by low-altitude polar orbiting satellites (Burch, 1968), the cusp has been considered an easy-to-access local "hole" around the magnetic neutral region (not as a point but an area) where the magnetic barrier is so small that the magnetosheath plasma may access independently of the global energy/momentum transfer through the other magnetospheric boundaries. Intensive statistical studies to date (e.g., Newell and Meng, 1992; 1994) have shown that the cusp is indeed a narrow and persistent region near local noon. The question then is how to theoretically inject the bulk magnetosheath plasma into the narrow ionospheric cusp.

Spreiter and Summers (1967) proposed to attach an indentation region in their gas-dynamics magnetosheath simulation to allow stagnant particle injection into the magnetic cusp. Such stagnant cusp has been observed during weak interplanetary magnetic field (IMF) conditions without internal convection signatures (Lundin et al., 1991). Later, importance of turbulence for the plasma access was proposed after Heos-2 and Interball-1 found highly turbulent region near the outer cusp (Paschmann et al., 1976; Haerendel et al., 1978; Savin et

al., 1997). Direct plasma access by a bulk deceleration is also considered using attached shock (Walters, 1966), magnetic tension force (Crooker, 1979), and the mass loading effect of the escaping ionospheric ions in the de-Laval nozzle-like geometry of the exterior cusp (Yamauchi and Lundin, 1997). These direct entry models ("turbulent/diffusive entry" and "direct flowing entry" models, respectively) require non-MHD and non-adiabatic processes in the local cusp. Note that the direct entry models may allow an independent global open mechanism rest of the magnetopause.

A quite different view is provided from magnetohydrodynamics (MHD): the magnetosphere is completely divided into either open or closed but nothing in between, even near the cusp neutral region; i.e., the cusp is just a part of the global open region (Reiff et al., 1977; Cowley et al., 1991; Lockwood et al., 1995; Onsager and Elphic, 1996). This global MHD view includes both pure MHD models and MHD-drift models (use linear drift trajectory inside the magnetosphere). Because of its one-fluid treatment, the MHD models predict only one global singularity or openness (i.e., source of the dayside magnetospheric convection) regardless of the IMF condition (Crooker, 1988; Hill, 1994). Even after modifying MHD using the cusp neutral region (Crooker et al. 1998), the MHD simulations still predict only one "driving" point of the convection in each hemisphere in dayside, rejecting the idea of local independency for the cusp.

2. Differences of the cusp models

Although many observational "tests" have been performed for specific mod- els, we are yet lacking a comparative examination of different cusp models against observations. There are some difficulties for such examination.

First, the differences between various cusp models are not well under- stood. All models require a magnetic singularity and an open configuration in the local cusp, but the reasons for this openness are quite different between models. Therefore, the differences can never be understood by simply drawing the magnetic field lines. The main difference lies on how to under- stand the cusp singularity in the global magnetospheric configuration, and it can be summarised as how to draw the cusp configuration in zero-order and first-order approximations. The zero-order approximations for major cusp models are illustrated in Figure 1. (a) The MHD models (including MHD-drift models) first draw the magnetic field lines (via MHD modeling) and add the plasma motion and waves later. (b) The turbulence/diffusive entry models first draw the region of turbulence without solid magnetic field or flow direction. (c) The direct flowing entry models first draw the fluid motion (and boundaries) and add turbulent regions and magnetic field lines if possible.

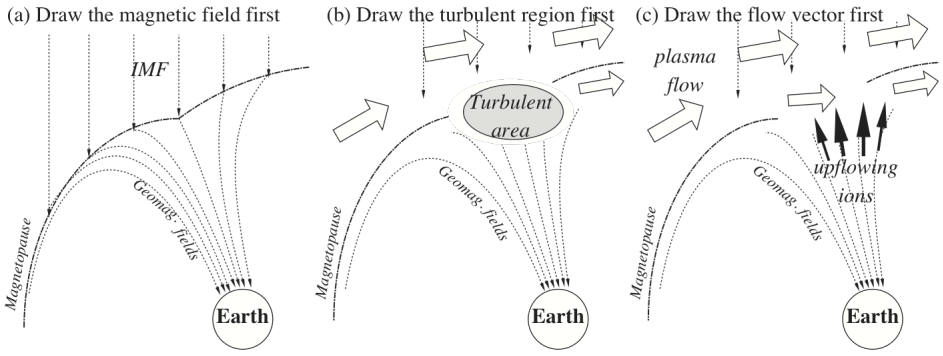

Figure 1. Three main categories of cusp models classified by the zero-order approximation. (a) The reconnection models. (b) The turbulence/diffusive entry models. (c) The direct flowing entry models.

Second, all models predict very similar cusp features. For example, both energetic and low-energy ions are predicted at different places in the cusp after the injected ions are affected by very active waves and electric field (e.g., Pottelette et al., 1990). All models also predict a bulk flow near the Alfvén speed in the magnetospheric rest frame, which is similar to "Cowley- D" distribution (Lockwood et al., 1995) within the observational accuracy. Therefore, MHD-drift simulations, which succeeded reproducing some cusp observation (e.g., Lockwood et al., 1995; Onsager and Elphic, 1996) eventually support the direct entry models as well, by simply adjusting the simulation parameters within realistic values. What we need is to extract the qualitative differences of various models, and to test them against a large body of observations. Without such procedure, one may not call a "quantitative" comparison as a "test."

Third, the cusp has very variable morphologies (Yamauchi and Lundin, 1994), and hence individual case studies are often misleading. Just finding a signature of one mechanism does not tell anything about the major mechanism because more than two processes may take place simultaneously (this is very likely with the cusp). For example, the observation of sunward flow burst at high-altitude during northward IMF (Kessel et al., 1996) does not mean that such a flow exists always in the major part of the cusp; in fact the sunward flow burst covers only a small part of the cusp in both space and time (Woch and Lundin, 1992; Yamauchi and Lundin, 1994).

Finally, we need high-resolution data for comparison. Although MHD-drift models have been successful in predicting simplified dayside observations such as the ionospheric convection and the particle energy-latitude (E-L) and pitch-angle (P-A) dispersions, the consistency is found only for low-resolution observations, but not for high-resolution ones.

One such example is the ionospheric convection (Yamauchi et al., 2000). Since the convection pattern is equivalent to integration (i.e., smoothing) of the field-aligned current (FAC) distribution, the ionospheric convection observed by ground instruments smears away

the fine FAC structures such as the boundaries between the merging cell and the lobe cell. The MHD models predict such a smeared cusp convection as a part of global convection, but they have been unsuccessful in explaining the extra FAC sheets and corresponding convection cells (Burch et al., 1985; Taguchi et al., 1993) obtained from high-resolution satellite observations. The observations instead indicate the independency of the cusp local convection predicted by the direct entry models.

To overcome the difficulties listed above, this paper attempts a systematic comparison of cusp models by listing differences of the models, and by listing low- and high-resolution observations against the predictions of these models. Table 1 summarizes the main differences of three major cusp models obtained from various references. From this summary one can make qualitative predictions, which are to be compared with observations.

Table I. Assumptions and predictions of major cusp models (*1)

Models	MHD(+drift)(*2)	Diffusive/Turbulent entry(*3)	Direct flowing entry(*4)
Zero-order config. (cf. Figure 1)	**B** is given, **u** and **W** are added	**W** is given, **u** and **B** are added	**u** is given, **B** and **W** are added
ion escape	ignored	some role for turbulence	major role (mass-loading)
injecting plasma trajectory	MHD (M'sheath) & drift (M'sphere)	non-MHD/non-adiabatic due to turbulence	non-MHD/non-adiabatic for shocked flow
fluid elements	one fluid	one fluid	multi-fluids
energy distribution	Maxwellian	non-Maxwellian	non-Maxwellian
cusp convection	part of global convection	independent of global convection (turbulent)	independent of global convection
wave & turbulence	not important	essential	important
location of dynamo (FAC)	downstream (region 0 for IMF $\mathbf{B_Z} < 0$)	inside the turbulent region	upstream (region 1 for IMF $\mathbf{B_Z} < 0$)
ion energization by	B-tension	turbulence	compression or shock
e^- energization (for auroral e^-)	M'sheath e^- (thermal e^-)	by turbulence in the outer cusp	by Alfvén waves above the ionosphere
role of M-I coupling	M'sphere determines ionosphere	some turbulence comes from ionosphere	essential (e.g., to steepen the shock)
auroral repetition	instability at M'pause	eigen oscillation	M-I coupling
meso-scale injections	no overlap except by finite gyroradii (*5)	sometimes overlaps sometimes not	sometimes overlaps sometimes not

*1) We use the following abbreviations (in addition to those defined in the text): **B** (magnetic field); **u** (flow velocity); **W** (region of wave activity); e^- (electrons); M' (magneto-); M-I (magnetosphere-ionosphere).
*2) Reiff et al., 1977; Crooker, 1988; Cowley et al., 1991; Hill, 1994; Onsager and Elphic, 1996; Lockwood, 1998; Crooker et al., 1998.
*3) Reiff et al., 1977; Haerendel et al., 1978; Heikkila, 1985; Savin et al., 1997.
*4) Walter, 1966; Spreiter and Summers, 1967; Yamauchi and Lundin, 1997; Yamauchi et al., 2000.
*5) re-reconnection does not explain the Viking/Freja observations of overlapping injections (Yamauchi et al., 1995).

3. Low resolution observations

We first compare the model predictions with low-resolution observations which were established a decade ago (Heikkila and Winningham, 1971; Friis-Christensen et al., 1975; Reiff et al., 1977; Hill and Reiff, 1977; Dan- dekar and Pike, 1978; Iijima et al., 1978; McDiarmid et al., 1979; Burch et al., 1982; Clauer and Banks, 1986; Sandholt et al., 1986; Heppner and Maynard, 1987; Newell et al., 1989; Kremser and Lundin, 1990; Knipp et al., 1991; Woch and Lundin, 1992; Newell and Meng, 1992; and references therein). They are:
(*l-1*) drastic change of the cusp morphology between northward and southward IMF;
(*l-2*) IMF BY dependence of the cusp location, convection, and field;
(*l-3*) Decreasing E-L dispersion with latitude;
(*l-4*) V-shaped P-A dispersion indicating non-stagnant injections;
(*l-5*) accelerated component of the magnetosheath plasma in the boundary cusp;
(*l-6*) two-cell convection pattern with the cusp inside the merging cell;
(*l-7*) enhanced convection ("throat") near the cusp;
(*l-8*) two or at most three FAC sheets in the cusp meridian;
(*l-9*) magnetosheath plasma in the cusp region 0 (C-0) and cusp region 1 (C-1) FACs;
(*l-10*) quick response to IMF changes;
(*l-11*) structured and energized electrons in the boundary cusp;
(*l-12*) structured red aurora (630 nm) and its poleward motion (PMAF) every several minutes; and (*l-13*) midday gap of the cusp red aurora.

Table 2: Comparison of major cusp models with low-resolution data

observations	MHD(+drift)	Diffusive/Turbulent	Direct flowing
l-1. IMF B_Z dependence	predicted	may be consistent	predicted
l-2. IMF B_Y dependence	predicted	predicted	predicted
l-3. energy-latitude dispersion	predicted	may be consistent	predicted
l-4. pitch-angle dispersion	predicted	may be consistent	may be consistent
l-5. proton acceleration	predicted	predicted	predicted
l-6. two-cell convection	predicted	may be consistent	may be consistent
l-7. convection throat	predicted	difficult	predicted
l-8. FAC sheets = 2 or 3	predicted	may be consistent	difficult
l-9. FAC with M'sheath ions	predicted	predicted	predicted
l-10. quick response	predicted	may be consistent	predicted
l-11. structured electrons	predicted	predicted	predicted
l-12. PMAF	predicted	may be consistent	predicted
l-13. midday gap	difficult	difficult	predicted

Table 2 summarizes the comparison of three major cusp models with these low-resolution data. The model predictions are taken from the references listed in Table 1. While MHD models seem to have the best support in Table 2, this is not the case with high-resolution observations.

4. Some unreported features

Before summarizing high-resolution observations, we show some important but not yet published cusp features. Figure 2 shows a Viking dayside traversal, which contains a typical stagnant cusp (at 80 − 81°) and a temporal injection (at 76°) equatorward of the cusp. IMF is northward during both injections.

One can easily notice the differences between the equatorward injection and the main cusp in their morphology (E-L dispersion) and detailed characteristics such as P-A dispersion, energy-broadening (= temperature), and meso-scale substructures. P-A dispersion in the cusp is not strictly V- shaped (plasma influx at 0° P-A is much smaller than that at 90° P-A), contrary to the equatorward injection. The difference is also recognized in the sharpness of the upper energy cut-off (corresponding to temperature). These differences make the spectrogram of the equatorward injection "clear" compared to the cusp injections. Such a clear dispersion pattern is observed only outside the cusp according to all Viking data (nearly 900 cusps with 400 cusp propers). Hence, (1) the equatorward injection is not a transient cusp, and (2) the energy, E-L, and P-A dispersions in the cusp are already strongly modified (by e.g., wave or turbulence).

The lack of field-aligned component in the cusp proper is a common feature in all Viking cusp observations. Such quasi-V-shaped P-A dispersion is no longer the evidence for non-stagnant injection, and the dispersion cannot be used to estimate the source distance (cf. Reiff et al., 1977). The source-distance calculation is possible only if the injected plasma have not experienced any wave-particle interaction, thermalization, or field-aligned potential drop. Such a clean case is seen at 1340-1346 UT in this figure, which gives us the source distance of < 10 Re.

The main cusp at 1350-1355 UT is composed of several meso-scale injections, forming a stagnant cusp as a whole. The average energy of the ions is about 300 eV, which is somewhat lower than that of the equatorward injection and typical magnetosheath plasma, indicating a bulk deceleration of injecting plasma. Such a deceleration feature is always seen in the cusp proper regardless of the IMF directions, although energized ions are often seen in the boundary cusp where the wave/turbulence activities are extremely high (Woch and Lundin, 1992).

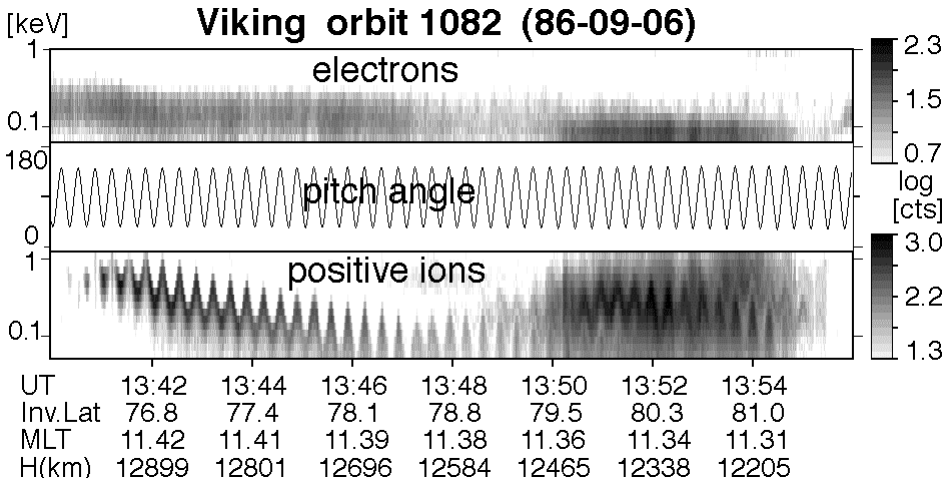

Figure 2. Viking ion and electron energy spectrogram for orbit 1082 (6 September, 1986).

The E-L dispersion at a given pitch angle provides some information about the convection velocity. Inside the cusp proper in Figure 2, the dispersion is nearly flat or slightly decreasing toward the pole, indicating that the poleward convection must be very slow, in agreement with Woch and Lundin (1992). There is no signature of sunward dispersion, which is required for the high-latitude reconnection or the MHD models. Thus the central part of the cusp is not a simple downstream of the boundary cusp (Yamauchi and Blomberg, 1997).

5. High resolution observations

We now list the high-resolution observations, and compare them to the MHD and the direct flowing entry models. We limit our discussion to low- latitude observations which we currently have sufficient data available:

(h-1) The cusp morphology (shape, size, E-L dispersion, acceleration) is quite various for the same solar wind (SW) conditions (Yamauchi and Lundin, 1994);

(h-2) The cusp morphology depends drastically on the SW dynamic pressure compared to the IMF BZ dependence (Newell and Meng, 1994);

(h-3) The average proton energy in the cusp is lower than that in the magnetosheath (cf. Figure 2);

(h-4) Energetic (~ 102 keV) particles are constantly found (Kremser et al., 1995; Chen et al., 1998);

(h-5) The cusp proper is not continuous to its surroundings for the plasma population, flux, E-L dispersion (or lower energy cut-off), and the convection velocity (Kremser and Lundin, 1990; Woch and Lundin, 1992; Yamauchi and Blomberg, 1997);

(h-6) C-1 and C-0 FACs are strongest at the boundary of the cusp proper but not inside it (Yamauchi et al., 2000);

(h-7) The P-A distribution lacks the field-aligned component (cf. Figure 2);
(h-8) Tailward convection slows down and is strongly deflected to east-west direction inside the cusp proper (Woch and Lundin, 1992; Yamauchi and Blomberg, 1997);
(h-9) While the boundary cusp (cleft) sometimes moves poleward together with convection (i.e., jumps equatorward for next injection), the cusp proper is relatively stationary (i.e., its equatorward motion is continuous) regardless of the convection during southward IMF (Nilsson et al., 1996);
(h-10) For finite IMF BY , an extra "independent" convection cell appears in the cusp, together with corresponding four FAC sheets (region 2 (R-2), region 1 outside the cusp (R-1), C-1, and C-0) on the same meridian in either prenoon or postnoon (Burch et al., 1985; Taguchi et al., 1993; Yamauchi et al., 2000);
(h-11) The relative intensities of C-1 and R-1 FACs are independent to each other (Yamauchi et al., 2000); (h-12) C-1 FAC $\geq$ C-0 FAC for southward IMF and C-1 FAC $\leq$ C-0 FAC for northward IMF (Potemra, 1994; Yamauchi et al., 1998);
(h-13) Waves and turbulence (including the standing Alfv´en wave) are most intensified at the boundary cusp (Pottelette et al., 1990; Peterson et al., 1993);
(h-14) The cusp red aurora is structured for southward IMF but is diffuse for weak IMF, and both types of aurora may coexist (Sandholt, 1997);
(h-15) The structured cusp red aurora is most likely caused by the superthermal electrons, which are generated by kinetic/inertia Alfv´en waves just above the ionosphere (Chaston et al., 1999);
(h-16) The cusp is embedded with many meso-scale injections, which are sometimes stepping without overlap and sometimes overlapped beyond the finite gyroradii distance (Escoubet et al., 1992; Yamauchi and Lundin, 1994; Norberg et al., 1994; Yamauchi et al., 1995);
(h-17) The meso-scale FACs are not forming but just embedded to large-scale FACs in the cusp proper, whereas R-1 FAC are sometimes composed of several intense meso-scale FACs associated with electron bursts (Yamauchi et al., 2000);
and (h-18) The particle precipitation and FACs are subject to extremely strong seasonal variation compared to the other dayside part or the cross-polar potential drop during large IMF BY (Newell and Meng, 1988; Yamauchi and Araki, 1989; Lu et al., 1994).

Apparently some "examination" results from the low-resolution comparison (Table 2) are no longer valid after the high-resolution comparison, such as l-3 (replaced to h-1, h-5, h-16), l-4 (to h-7), l-5 (to h-4, h-5), l-6, l-7, l-8, (all replaced to h-10), l-9 (to h-6, h-11, h-17), and l-12 (to h-14, h-15). The summary of the high-resolution, Table 3, does not include the source distance estimation from the large-scale E-L dispersion or the P-A distribution because one may not make such an estimate after the high-resolution observations (cf. h-9, h-16, and h-7) showed completely different dispersion features.

Table 3: Comparison of two types cusp models with high-resolution data

observations	MHD(+drift)	Direct flowing
h-1. variety of the morphology	difficult	predicted
h-2. SW dynamic pressure dependence	may be consistent	predicted
h-3. proton deceleration feature	difficult	predicted
h-4. 10^2 keV particles	difficult	predicted
h-5. discontinuous at cusp boundary	difficult	predicted
h-6. FAC at cusp boundary	predicted	predicted
h-7. fine pitch-angle distribution	may be consistent	may be consistent
h-8. convection blockage and deflection	difficult	predicted
h-9. slipping convection against cusp	difficult	predicted
h-10. extra convection cell and 4-sheet FAC	difficult	predicted
h-11. independency of R-1 and C-1	may be consistent	predicted
h-12. C-1/C-0 asymmetry	difficult	predicted
h-13. wave/turbulence at cusp boundary	may be consistent	predicted
h-14. two types of cusp red aurora	may be consistent	predicted
h-15. electron source for cusp aurora	may be consistent	predicted
h-16. overlapping injections	difficult	predicted
h-17. meso-scale FACs	may be consistent	predicted
h-18. seasonal variation	difficult	predicted

Although the direct flowing models received good support in Table 3, we cannot conclude anything about this model because the table contains only low-altitude observations. We need further examination with higher- resolution data and in-situ (high-altitude) observations in future before concluding anything. With this note in mind, we may state that MHD models do not account for many high-resolution cusp observations, and that the cusp is most likely an independent locally open region.

6. Conclusion

We have thoroughly compared low-altitude observations with two of major cusp models (MHD models and direct flowing entry models). Although low-resolution data agrees with MHD models, high-resolution data mostly contradicts them. Thus, “test” must be performed with high-resolution data when considering even the large-scale phenomena, and comparison with low-resolution data can be misleading. MHD is certainly successful in drawing the global configuration of the magnetosphere. However, this global nature makes MHD an unsuitable assumption in the cusp special geometry, as is discussed in Yamauchi and Blomberg (1997).

Acknowledgements

The Viking project is supported by the Swedish National Space Board.

References

Burch, J.L. (1968) Low-energy electron fluxes at latitudes above the auroral zone, J. Geophys. Res., 73, 3585.

Burch, J.L., Reiff, P.H., Heelis, R.A., et al. (1982) Plasma injection and transport in the mid-altitude polar cusp, Geophys. Res. Lett., 9, 921.

Burch, J.L., Reiff, P.H., Menietti, J.D., et al. (1985) IMF BY dependent plasma flow and Birkeland currents in the dayside magnetosphere 1. dynamics explorer observations, J. Geophys. Res., 90, 1577.

Chaston, C.C., Carlson, C.W., Peria, W.J., et al. (1999) FAST observations of inertial Alfven waves in the dayside aurora, Geophys. Res. Lett., 26, 647.

Chen, J., Frits, T.A., Sheldon, R.B., et al. (1998) Cusp energetic particle events, J. Geophys. Res., 103, 69.

Clauer, C.R. and Banks, P.M. (1986) Relationship of the interplanetary electric field to the high-latitude ionospheric electric field and currents: Observations and model simulation, J. Geophys. Res., 91, 6959.

Cowley, S.W.H., Morelli, J.P., and Lockwood, M. (1991) Dependence of convective flows and particle precipitation in the high-latitude dayside ionosphere on the X and Y components of the interplanetary magnetic field, J. Geophys. Res., 96, 5557.

Crooker, N.U. (1979) Dayside merging and cusp geometry, J. Geophys. Res., 84, 951. Crooker, N.U. (1988) Mapping the merging potential from the magnetopause to the ionosphere through the dayside cusp, J. Geophys. Res., 93, 7338.

Crooker, N.U., Lyon, J.G., and Fedder, J.A. (1998) MHD model merging with IMF BY : Lobe cells, sunward polar cap convection, and overdraped lobes, J. Geophys. Res., 103, 9143.

Dandekar, B.S. and Pike, C.P. (1978) The midday discrete auroral gap, J. Geophys. Res., 83, 4227.

Escoubet, C.P., Smith, M.F., Fung, S.F., et al. (1992) Staircase ion signature in the polar cusp: A case study, Geophys. Res. Lett., 19, 1735.

Friis-Christensen, E. and Wilhjelm, J. (1975) Polar cap currents for different directions of the interplanetary magnetic field in the Y-Z plane, J. Geophys. Res., 80, 1248.

Haerendel, G., Paschmann, G., Sckopke, N., et al. (1978) The frontside boundary layer of the magnetosphere and the problem of reconnection, J. Geophys. Res., 83, 3195.

Heikkila, W.J. and Winningham, J.D. (1971) Penetration of magnetosheath plasma to low altitudes through the dayside magnetospheric cusps, J. Geophys. Res., 76, 883.

Heikkila, W.J. (1985) Definition of the cusp, In J.A. Holtet and A. Egeland, editors The Polar Cusp, 387, D. Reidel Pub.

Heppner, J.P. and Maynard, N.C. (1987) Empirical high-latitude electric field models, J. Geophys. Res., 92, 4467.

Hill, T.W. (1994) Theoretical models of polar-cap convection under the influence of a northward interplanetary magnetic field, J. Atmos. Terr. Phys., 56, 185

Hill, T.W. and Reiff, P.H. (1977) Evidence of magnetospheric cusp proton acceleration by magnetic merging at the dayside magnetopause, J. Geophys. Res., 82, 3623.

Iijima, T., Fujii, R., Potemra, T.A., and Saflekos, N.A. (1978) Field-aligned currents in the south polar cusp and their relationship to the Interplanetary magnetic field, J. Geophys. Res., 83, 5595.

Kessel, R.L., Chen, S.-H., Green, J.L., et al. (1996) Evidence of high-latitude reconnection during northward IMF; Hawkeye observations, Geophys. Res. Lett., 23, 583.

Knipp, D.J., Richmond, A.D., Emery, B., et al. (1991) Ionospheric convection response to changing IMF direction, Geophys. Res. Lett., 18, 721.

Kremser, G., Woch, J., Mursula, K., et al. (1995) Origin of energetic ions in the polar cusp inferred from ion composition measurements by the Viking satellite, Ann. Geophys., 13, 595.

Kremser, G. and Lundin, R. (1990) Average spatial distributions of energetic particles in the mid-altitude cusp/cleft region observed by Viking, J. Geophys. Res., 95, 5753.

Lockwood, M., Davis, D.J., Smith, M.F., et al. (1995) Location and characteristics of the reconnection X line deduced from low-altitude satellite and ground-based observations 2. Defense Meteorological Satellite Program and European Incoherent Scatter data,

J. Geophys. Res., 100, 21803. Lockwood, M. (1998) Identifying the open-closed field line boundary, In J. Moens et al., editors, Polar Cap Boundary Phenomena, 73, Kluwer Acad. Pub.

Lu, G., Richmond, A.D., Emery, B.A. et al. (1994) Interhemispheric asymmetry of the high-latitude ionospheric convection pattern, J. Geophys. Res., 99, 6491.

Lundin, R., Woch, J., and Yamauchi, M. (1991) The present understanding of the cusp, ESA-SP, 330, 83.

McDiarmid, I.B., Burrows, J.R., and Wilson, M.D. (1979) Large-scale magnetic field perturbations and

particle measurements at 1400 km on the dayside, J. Geophys. Res., 84, 1431.
Newell, P.T. and Meng, C.-I. (1988) Hemispherical asymmetry in cusp precipitation near solstices, J. Geophys. Res., 93, 2643.
Newell, P.T. and Meng, C.-I. (1992) Mapping the dayside ionosphere to the magnetosphere according to particle precipitation characteristics, Geophys. Res. Lett., 19, 609.
Newell, P.T. and Meng, C.-I. (1994) Ionospheric projections of magnetospheric regions under low and high solar wind pressure conditions, J. Geophys. Res., 99, 273.
Newell, P.T., Meng, C.-I., Sibeck, D.G., and Lepping, R. (1989) Some low-altitude cusp dependencies on the interplanetary magnetic field, J. Geophys. Res., 94, 8921.
Nilsson, H., Yamauchi, M., Eliasson, et al. (1996) The ionospheric signature of the cusp as seen by incoherent scatter radar, J. Geophys. Res., 101, 10947.
Norberg, O., Yamauchi, M., Eliasson, L., and Lundin, R. (1994) Freja observations of multiple injection events in the cusp, Geophys. Res. Lett., 21, 1919.
Onsager, T.G. and Elphic, R.C. (1996) Is magnetic reconnection intrinsically transient or steady state? the Earth's magnetopause as a laboratory, EOS, 77, 241.
Paschmann, G., Haerendel, G., Sckopke, N., and Rosenbauer, H. (1976) Plasma and field characteristics of the distant polar cusp near local noon: The entry layer, J. Geophys. Res., 81, 2883.
Peterson, W.K., Abe, T., Andre, M., et al. (1993) Observations of a transverse magnetic field perturbation at two altitudes on the equatorward edge of the magnetospheric cusp, J. Geophys. Res., 98, 21463.
Potemra, T.A. (1994) Sources of large-scale Birkeland currents, In J.A. Holtet, and A. Egeland, editors, Physical Signatures of Magnetospheric Boundary Layer Processes, 3, Kluwer Acad. Pub.
Pottelette, R., Malingre, M., Dubouloz, N., et al. (1990) High-frequency waves in the cusp/cleft regions, J. Geophys. Res., 95, 5957.
Reiff, P.H., Hill, T.W., and Burch, J.L. (1977) Solar wind plasma injection at the dayside magnetospheric cusp, J. Geophys. Res., 82, 479.
Sandholt, P.E., Deehr, C.S., Egeland, A., et al. (1986) Signatures in the dayside aurora of plasma transfer from the magnetosheath, J. Geophys. Res., 91, 10063.
Sandholt, P.E. (1997) Dayside polar cusp/cleft aurora: morphology and dynamics, Phys. Chem. Earth, 22, 675.
Savin, S.P., Romanov, S.A., Fedorov, A., et al. (1997) The cusp/magnetosheath interface on May 29, 1996: Interball-1 and Polar observations, Geophys. Res. Lett., 25, 2963.
Spreiter, J.R. and Summers, A.L. (1967) On conditions near the neutral points on the magnetosphere boundary, Planet. Space Sci., 15, 787.
Taguchi, S., Sugiura, M., Winningham, J.D., and Slavin, J.A. (1993) Characterization of the IMF BY - dependent field-aligned currents in the cleft region based on DE 2 observations, J. Geophys. Res., 98, 1393.
Walters, G.K. (1966) On the existence of a second standing shock wave attached to the magnetosphere, J. Geophys. Res., 71, 1341.
Woch, J. and Lundin, R. (1992) Magnetosheath plasma precipitation in the polar cusp and its control by the interplanetary magnetic field, J. Geophys. Res., 97, 1421.
Yamauchi, M., and Araki, T. (1989) The interplanetary magnetic field BY-dependent field-aligned current in the dayside polar cap under quiet conditions, J. Geophys. Res., 94, 2684.
Yamauchi, M. and Lundin, R. (1994) Classification of large-scale and meso-scale ion dispersion patterns observed by Viking over the cusp-mantle region, In J.A. Holtet, and A. Egeland, editors, Physical Signatures of Magnetospheric Boundary Layer Processes, 99, Kluwer Acad. Pub.
Yamauchi, M. and Lundin, R. (1997) The wave-assisted cusp model: Comparison to low-altitude observations, Phys. Chem. Earth, 22, 729.
Yamauchi, M. and Blomberg, L. (1997) Problems on Mappings of the Convection and on the Fluid Concept, Phys. Chem. Earth, 22, 709.
Yamauchi, M., Lundin, R., and Potemra, T.A. (1995) Dynamic response of the cusp morphology to the IMF changes: An example observed by Viking, J. Geophys. Res., 100, 7661.
Yamauchi, M., Lundin, R., Eliasson, L., et al. (1998) Relationship between large-, meso, and small-scale field-aligned currents and their current carriers, In J. Moens et al., editors, Polar Cap Boundary Phenomena, 173, Kluwer Acad. Pub.
Yamauchi, M., Lundin, R., Eliasson, L., et al. (2000) Independency of the Dayside Field-Aligned Current System: A Restriction to Cusp Models, in "Magnetospheric Current System", Geophys. Monograph, 118, edited by S. Ohtani, R. Fujii, M. Hesse, and R.L. Lysak, 245-252, 2000.